Scaling and energy transfer in rotating turbulence

Wolf-Christian Müller[1] and Mark Thiele[2,1]

[1] *Max-Planck-Institut für Plasmaphysik, 85748 Garching, Germany*[*]
[2] *Universität Bayreuth, Theoretische Physik II, 95440 Bayreuth, Germany*[†]

The inertial-range properties of quasi-stationary hydrodynamic turbulence under solid-body rotation are studied via high-resolution direct numerical simulations. For strong rotation the nonlinear energy cascade exhibits depletion and a pronounced anisotropy with the energy flux proceeding mainly perpendicularly to the rotation axis. This corresponds to a transition towards a quasi-two-dimensional flow similar to a linear Taylor-Proudman state. In contrast to the energy spectrum along the rotation axis which does not scale self-similarly, the perpendicular spectrum displays an inertial range with $k_\perp^{-2}$-behavior. A new phenomenology gives a rationale for the observations. The scaling exponents ζ_p of structure functions up to order $p = 8$ measured perpendicular to the rotation axis indicate reduced intermittency with increasing rotation rate. The proposed phenomenology is consistent with the inferred asymptotic non-intermittent behavior $\zeta_p = p/2$.

PACS numbers: 47.32.-y;47.27.Gs;47.27.E-;47.27.ek

The inherent properties of turbulence in a rotating reference frame are important for, e.g., the dynamics of atmosphere and oceans, liquid planetary cores, and engineering problems. The nonlinear spectral transfer of energy by the direct turbulent cascade and the associated energy spectrum are particularly interesting due to their direct connection to the dynamical processes governing rotating turbulence. Most of the available experimental data [1–5] yields no conclusive information on the expected self-similar scaling of the energy spectrum in the inertial range of scales and its dependence on the rotation frequency Ω. Although recent experiments [6–8] have shed some light on these issues, the scaling of two-point statistics in rotating turbulence remains a controversial topic.

Direct numerical simulations [9–16] and large-eddy simulations, see e.g. [17–19], have been carried out only at low and moderate Reynolds numbers precluding clear scaling observations. Nevertheless, most of the cited works agree in that the nonlinear spectral transfer of energy to smaller scales diminishes with growing Ω, accompanied by a transition of the flow towards a quasi-two-dimensional state perpendicular to the fixed rotation axis, $\boldsymbol{\Omega}$. The transition manifests itself in an increasing ratio of integral length scales parallel and perpendicular to $\boldsymbol{\Omega} = \Omega\hat{\boldsymbol{e}}_3$, defined as $L_{i,j} = \int_0^{L_\infty} \mathrm{d}\ell \langle v_i(\boldsymbol{r}) v_i(\boldsymbol{r} + \ell\hat{\boldsymbol{e}}_j)\rangle / \langle v_i^2(\boldsymbol{r})\rangle$, L_∞ representing the largest possible distance between two points in the simulation volume and ℓ denoting the respective space increment.

This Letter presents high-resolution direct numerical simulations of incompressible rotating homogeneous turbulence driven at largest scales and proposes a phenomenology of the energy cascade which suggests a physical explanation for the observed attenuation of nonlinear spectral transfer under the influence of rotation. In addition, the model gives a rationale for the observed trend towards two-dimensionality in rapidly rotating turbulence which is corroborated by the simulations. The scaling of two-point structure functions perpendicular to $\boldsymbol{\Omega}$ indicates a decreasing level of intermittency with growing Ω.

Incompressible hydrodynamic turbulence under solid-body rotation is usually described by the Navier-Stokes equations including the Coriolis force [20] given here in dimensionless form with the vorticity, $\boldsymbol{\omega} = \nabla \times \boldsymbol{v}$, and the non-dimensional kinematic viscosity μ and rotation frequency $\Omega = |\boldsymbol{\Omega}|$,

$$\partial_t \boldsymbol{\omega} = \nabla \times (\boldsymbol{v} \times \boldsymbol{\omega} + 2\boldsymbol{v} \times \boldsymbol{\Omega}) + \mu \Delta \boldsymbol{\omega}\,, \tag{1}$$

$$\nabla \cdot \boldsymbol{v} = 0\,. \tag{2}$$

Equations (1) and (2) are numerically integrated using an explicit trapezoidal leapfrog scheme [21] with the diffusive term included by an integrating factor, see e.g. [22], while the remaining right-hand-side of Eq. (1) is determined pseudospectrally. The simulation volume extends 2π in each dimension with triply periodic boundary conditions and a resolution of 512^3 collocation points. Aliasing errors are treated by spherical mode truncation [23]. Quasi-stationary turbulence is generated by a forcing which freezes all modes in a sphere of radius $k_f = 2$.

The initial state of the forced simulations is taken from non-rotating turbulence which has been freely decaying for about one large-eddy-turnover time, the period needed to reach the maximum of dissipation when starting with a smooth velocity field. This initial velocity field is characterized by an energy spectrum $E_k \sim \exp(-k^2/k_0^2)$, $k_0 = 4$, and random phases. Subsequently all Fourier modes with $k \leq 2$ are frozen. These modes sustain a gentle driving of the flow by nonlinear interaction with the fluctuating part of the system. As soon as total energy, $E = \int_V \mathrm{d}V v^2/2$, and dissipation, $\varepsilon = -\mu \int_V \mathrm{d}V \omega^2$, are statistically stationary with $E \simeq 1$ and $\varepsilon \simeq 0.25$ both mildly fluctuating, Ω is set to a finite value, 5 (system I) and 50 (system II).

The dimensionless kinematic viscosity μ is 4×10^{-4} in both cases. The characteristic length L_0 and velocity V_0, necessary for the calculation of macroscopic Rossby number, $\mathsf{Ro} = V_0/(2\Omega L_0)$, and Reynolds number, $\mathsf{Re} = L_0 V_0/\mu$, can only be determined a posteriori in homogeneous turbulence. Both quantities are estimated on dimensional grounds using E, ε, and Ω as $L_0 \sim E/(\Omega\varepsilon)^{1/2}$ and $V_0 \sim E^{1/2}$. Hence the Rossby and Reynolds number given in this paper are defined as $\mathsf{Ro} = \sqrt{\varepsilon/(4\Omega E)}$ and $\mathsf{Re} = \sqrt{E^3/(\Omega\varepsilon)}/\mu$, respectively. Note that another common estimate of the Rossby number is $\mathsf{Ro}^* = 4\mathsf{Ro}^2$.

After the sudden onset of rotation, E displays a sharp drop of about 20% (case I) and 13% (case II) with a subsequent remount that levels off near the previous state. The dissipation rate ε follows the general dynamics of energy, but does not increase again with $\varepsilon \simeq 0.05$ in both simulations. The observations can be understood by the rotation-induced depletion of the spectral energy transfer which causes a transient until forcing and cascade have reached a new equilibrium. The observed behavior does not differ qualitatively if the rotation is ramped up (as has been checked by test computations).

The following 15 (I) and 10 (II) large-eddy turnover times of statistically stationary rotating turbulence are characterized by $\mathsf{Ro} \simeq 5.3 \times 10^{-2}$, $\mathsf{Re} \simeq 4000$ (I) and $\mathsf{Ro} \simeq 1.3 \times 10^{-2}$, $\mathsf{Re} \simeq 2340$ (II). Perpendicular one-dimensional energy spectra, $E_{k_\perp} = \int \mathrm{d}k_\parallel \int \mathrm{d}k' |v_{\boldsymbol{k}}|^2/2$ with $k_\perp \perp \boldsymbol{\Omega}$, $k_\parallel \parallel \boldsymbol{\Omega}$, and k' perpendicular to $k_\perp$ and $k_\parallel$, are shown in Fig. 1. The spectrum of system I displays a scaling range for $4 \lesssim k_\perp \lesssim 20$ while in simulation II the dissipation region is starting at smaller k (see below). In addition, the spectrum of simulation II exhibits a bump around k_f where the forcing region descends into the freely evolving range of scales. This effect which is caused by the simple forcing scheme does not seem to significantly perturb the flow beyond $k \approx 5$. It is therefore tolerable at the chosen numerical resolution.

Although the inertial range in simulation II is shorter than in simulation I the perpendicular one-dimensional energy spectra in both cases exhibit scaling, $E_{k_\perp} \sim k_\perp^{-2}$, in agreement with direct numerical simulations at moderate Reynolds-number [12] and [13](for $k > k_f$), and shell-model calculations [24]. A formal analysis of the energy flux in helical mode decomposition [25] leads to the same result as well as dimensional analysis of the energy flux terms which occur in quasi-normal closure theories [26, 27] when assuming $\tau_* \sim \tau_\Omega \sim \Omega^{-1}$ for the relaxation timescale of nonlinear interactions, τ_*. The observed spectra are also in accord with one of several isotropic scalings proposed in weak-turbulence theory [28, 29]. However, this approach is only valid in the asymptotic limit $\tau_* \gg \tau_\Omega$ implying $k \ll k_\Omega$ (see below) which requires very strong rotation or an extremely broad inertial range and therefore is beyond the scope of the simulations considered here. In [13] k^{-3}-scaling is found at small wavenumbers in turbulence with medium-scale forcing. The observation is explained dimensionally by the missing explicit ε-dependence of the spectrum at large scales (also cf. [30] using a method based on reduced sets of nonlinear interactions). Recent experimental results [8] suggest an energy scaling exponent ≈ -2.5 for case II with the micro Rossby number of $\mathsf{Ro}_\omega = \langle\omega_3^2\rangle^{1/2}/(2\Omega) \simeq 0.08$ and an exponent of ≈ -1.7 for case I with $\mathsf{Ro}_\omega \simeq 0.7$. This disagreement is probably due to the different way of turbulence generation. While in the simulations there is a continuous large-scale forcing, turbulence in the experiment is exited initially and then subject to decay under rotation. In addition the experimental Rossby numbers are significantly larger than in our computations. The configuration is, therefore, not directly comparable to the simulations described here. This is also true for the experiment reported in [6] although the same scaling $\sim k^{-2}$ is observed there (however in an inverse energy cascade). It should be noted that the $k_\parallel$-dependence of the perpendicular energy spectrum (not shown) in our simulations confirms the expected concentration of energy around the plane $k_\parallel = 0$ [31, 32]. Furthermore, the perpendicular energy spectra at specific fixed $k_\parallel$ do not show clear spectral scaling. This is only seen in the sum $E_{k_\perp}$.

The energy spectra taken parallel to $\boldsymbol{\Omega}$ do not exhibit distinct scaling ranges. This is in accord with the strong rotation-induced decrease of the axis-parallel nonlinear energy flux (cf. Fig. 2), $T_{k_\parallel} = \int_0^{k_\parallel} \mathrm{d}k_\parallel \int \mathrm{d}k' \int \mathrm{d}k_\perp \left(i\boldsymbol{\omega}^* \cdot (\boldsymbol{k} \times \widetilde{[\boldsymbol{v} \times \boldsymbol{\omega}]}_{\boldsymbol{k}}) + c.c. \right) / \boldsymbol{k}^2$, with $\widetilde{[\bullet]}$ denoting Fourier transformation and $T_{k_\perp}$ defined analogously. Note that the Coriolis force has no direct effect on the kinetic energy since it is oriented perpendicularly to $\boldsymbol{v}$. It does, however, modify the nonlinear interactions leading to depletion and anisotropy of the energy cascade, cf. also [31, 32], which is apparent when regarding Fig. 2. All normalized transfer functions for $\Omega = 0$, 5, and 50 are negative throughout indicating a direct energy cascade towards small-scales. They show a damping of the energy flux at all scales with increasing Ω. The cascade depletion is much stronger in $T_{k_\parallel}$ than in $T_{k_\perp}$. Consequently, the cascade becomes highly anisotropic in the case of strong rotation which naturally leads to a dynamical two-dimensionalization of the flow. The transition towards 2D also manifests itself in the increasing ratio of parallel to perpendicular integral length scales with growing Ω where strong rotation, $\Omega = 50$, yields $L_{i,3}$ up to a factor 2.5 larger than $L_{i,1}$ and $L_{i,2}$ for $i = 1, 2, 3$. This trend is also seen in visualizations of the velocity field (not shown). The perpendicular longitudinal and lateral correlation lengths exhibit moderate systematic differences due to the forcing scheme which is not fully isotropic. This, however, does not cloud the main trend of two-dimensionalization in planes perpendicular to $\boldsymbol{\Omega}$.

The obtained results can be understood in the framework of a phenomenology of the energy cascade in rotating

turbulence which is set out in the following. While inertial waves present in rotating turbulence are undoubtedly an important dynamical process, the proposed picture of the energy cascade is based on the presumed energetic dominance of convective motions.

The wavenumber range strongly influenced by rotation lies above the scale at which the advection nonlinearity in Eq. (1) is roughly equal to the Coriolis force, $v_\ell^2/\ell \sim \Omega v_\ell$ where v_ℓ denotes an isotropically estimated velocity fluctuation at scale $\ell \sim k^{-1}$. Since non-rotating hydrodynamic turbulence exhibits Kolmogorov inertial-range scaling [33], $v_\ell \sim (\varepsilon\ell)^{1/3}$, one obtains the well-known rotation wavenumber [25, 34], $k_\Omega = (\Omega^3/\varepsilon)^{1/2}$, below which the energy cascade is modified by the Coriolis force acting in planes perpendicular to $\mathbf{\Omega}$.

The nonlinear energy transfer in those planes can be estimated dimensionally as $\varepsilon \sim v_\xi^2/\tau_{\rm tr}$ with the characteristic velocity fluctuation v_ξ in the axis-perpendicular plane at scale $\xi \sim k_\perp^{-1}$. Due to the lack of an inertial range in the direction parallel to $\mathbf{\Omega}$, a consequence of the quasi-2D-state, the approximation $E(\ell) \sim v_\xi^2$ suffices for the following scaling predictions. In isotropic non-rotating hydrodynamic turbulence fluid particles which belong to a turbulent structure at scale $\xi \sim \ell$ follow trajectories of length ξ for a turnover time, $\tau_{\rm tr} \sim \tau_{\rm NL} \sim \xi/v_\xi$, in the course of the energy cascade. When neglecting all nonlinearities fluid particles in rotating flows are displaced from the no-rotation trajectories in axis-perpendicular directions due to the Coriolis force and follow circular orbits of radius $r \sim v_\xi\tau_\Omega$ which close after $\tau_\Omega \sim \Omega^{-1}$. The nonlinear terms in Eq. (1) which dominate turbulence dynamics cause a strong deformation of the circular orbits. The deformed circles which we regard as abstract entities whose shapes can be left unspecified will be referred to as 'arcs'. Typically these do not close in themselves after τ_Ω but lead to an effective axis-perpendicular displacement $\sim r$ of the fluid particles. It is easy to verify that in the rotation dominated range of scales, $k < k_\Omega$, the displacement r is always smaller then ξ, requiring the fluid particles to perform ξ/r 'arc steps' to cover the distance ξ and to complete the cascade trajectory. In fact though, the direction in which a fluid particle is deflected by an arc movement is quasi-stochastic. Consequently, analogous to a random walk process $(\xi/r)^2$ arc steps are necessary to cover the distance ξ. Therefore, the nonlinear transfer time in the axis perpendicular direction is given by

$$\tau_{\rm tr} \sim \left(\frac{\tau_{\rm NL}}{\tau_\Omega}\right)^2 \tau_\Omega \,. \tag{3}$$

This result has also been obtained by formal analysis of the nonlinear energy flux [25] and in weak-turbulence theory [28]. We note in passing that the rotation-modified transfer time $\tau_{\rm tr}$ is larger than $\tau_{\rm NL}$ with $\tau_{NL} \sim \tau_{\rm tr}$ at k_Ω. From the previous it is clear that for $k \ll k_\Omega$ the turbulent energy cascade is highly anisotropic and progresses mainly in the direction perpendicular to the rotation axis in accord with the dynamic Taylor-Proudman theorem, see e.g. [16, 27]. The definition of τ_Ω used in this paper differs from the one known from weak turbulence theory which involves the ratio $k_\perp/k_\parallel$ (see, e.g., [28]). However, both definitions approach each other when $k_\perp/k_\parallel$ for the turbulent fluctuations does not depart strongly from unity as is the case here.

With relation (3) the dimensional estimate of the nonlinear energy flux is obtained as $\varepsilon \sim v_\xi^4/(\Omega\xi^2)$. Assuming $\varepsilon = $ const. throughout the inertial range yields a scaling law for the velocity fluctuations perpendicular to $\mathbf{\Omega}$,

$$v_\xi \sim (\Omega\varepsilon)^{1/4}\xi^{1/2} \,, \tag{4}$$

corresponding to the observed scaling of the energy spectrum $\sim k_\perp^{-2}$ [25, 26].

The rotation-dominated range of scales is limited from below by the wavenumber $\min(k_\Omega, k_d^\Omega)$ where k_d^Ω indicates approximate equality of nonlinear and dissipative energy-fluxes, $\varepsilon \sim \mu\xi^{-2}v_\xi^2$. Together with relation (4) this yields $k_d^\Omega \sim \mu^{-1}(\varepsilon/\Omega)^{1/2} \sim k_\Omega \frac{\varepsilon}{\mu\Omega^2}$. A different approach [25] leads to the same result. Since k_Ω grows and k_d^Ω diminishes with increasing Ω, there exists a critical rotation frequency for which the rotation-dominated regime has its largest extent, i.e. $R = \varepsilon/(\mu\Omega^2) = 1$. Higher rotation rates lead to a reduction of this range since $R < 1$. Here, for case I: $k_\Omega \simeq 50$, $k_d^\Omega \simeq 250$, $k_d \simeq 167$, $R \simeq 5$ and for case II: $k_\Omega \simeq 1581$, $k_d^\Omega \simeq 79$, $k_d \simeq 167$, $R \simeq 0.05$ which explains the shorter inertial range of $E_{k_\perp}$ in case II. The Kolmogorov dissipation wavenumber $k_d \sim (\varepsilon/\mu^3)^{1/4}$ roughly identifies the scale at which dissipation begins to dominate over the nonlinear energy flux.

At the given spatial resolution scaling exponents of the axis-perpendicular longitudinal velocity structure functions, $\langle|[\boldsymbol{v}(\boldsymbol{r}) - \boldsymbol{v}(\boldsymbol{r}+\boldsymbol{\xi})]\cdot\boldsymbol{\xi}/\xi|^p\rangle \sim \xi^{\zeta_p}$ can be determined for both systems up to order 8. However, the small inertial range for $\Omega = 50$ necessitates use of the extended self-similarity property (ESS) [35]. The relative exponents ζ_p/ζ_2 obtained via ESS approximately coincide with the ζ_p since relation (4) (in the non-intermittent limit) and the numerical result $E_{k_\perp} \sim k_\perp^{-2} = k_\perp^{-(\zeta_2+1)}$ suggest $\zeta_2 \approx 1$. The results shown in Fig. 3 are a sign of a gradual transition from the intermittent non-rotating case (represented by the She-Lévêque formula [36], $\zeta_p = p/9 + 2[1-(2/3)^{p/3}]$) towards a strongly rotating flow with weak intermittency. The observed reduction of intermittency is in accord with the expected

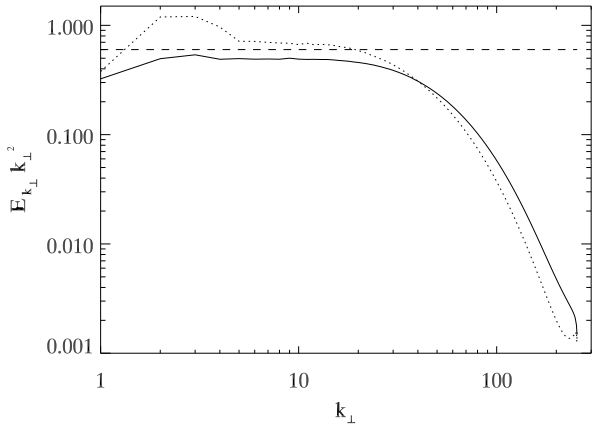

FIG. 1: One-dimensional energy spectra perpendicular to the rotation axis for different rotation frequencies. The spectra are time-averaged over 6 large-eddy turnover times and compensated with $k_\perp^2$ (solid line: $\Omega = 5$, dotted line: $\Omega = 50$).

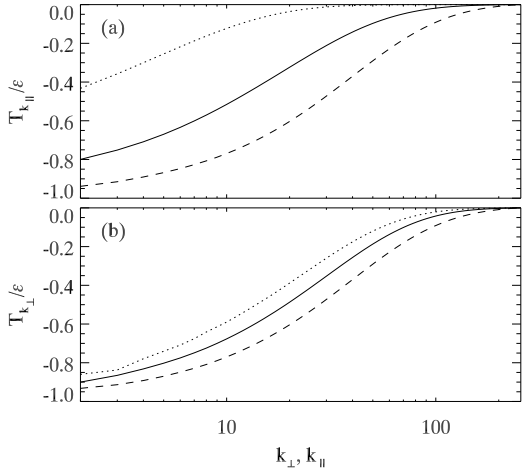

FIG. 2: Normalized and time-averaged nonlinear energy fluxes (a) parallel and (b) perpendicular to the rotation axis with $\Omega = 0$ (dashed line), $\Omega = 5$ (solid line), and $\Omega = 50$ (dotted line).

transition from strong fluid turbulence to weak inertial wave turbulence (see, e.g., [37]). The observations coincide with experimental findings given in [7] although in this experiment the flow is driven at small scales and in contrast to our simulations exhibits an inverse cascade of energy.

In summary, high-resolution direct numerical simulations of incompressible hydrodynamic turbulence driven at largest scales under moderate and strong rotation corroborate a proposed phenomenology of rotating turbulence which gives a simple rationale for the overall weakening of the energy cascade and the trend towards two-dimensional dynamics in rotating turbulent flows. Higher-order structure function scalings show a transition towards a non-intermittent state perpendicular to the rotation axis as known from 2D turbulence.

It is a pleasure to thank Friedrich Busse and Dieter Biskamp for helpful discussions.

* Electronic address: Wolf.Mueller@ipp.mpg.de
† Electronic address: Mark.Thiele@uni-bayreuth.de

[1] S. C. Traugott, Technical Note 4135, National Advisory Committee for Aeronautics, Washington, USA (1958).
[2] R. A. Wigeland, Ph.D. thesis, Illinois Institute of Technology (1978).
[3] A. Ibbetson and D. J. Tritton, Journal of Fluid Mechanics **68**, 639 (1975).

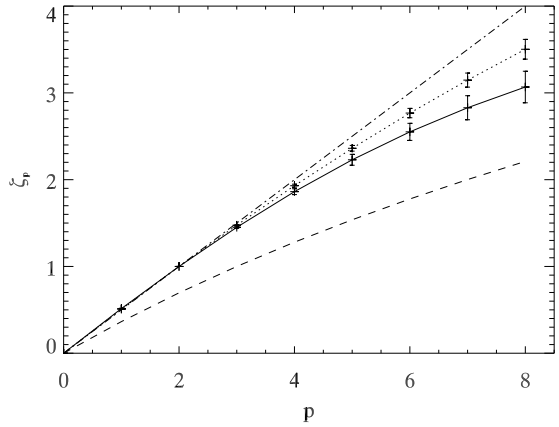

FIG. 3: Axis-perpendicular structure function scaling exponents ζ_p of velocity up to order 8 for moderate and strong rotation. Solid line: $\Omega = 5$, dotted line: $\Omega = 50$, dashed line: She-Lévêque intermittency model, dash-dotted line: non-intermittent scaling, $\zeta_p = p/2$.

[4] E. J. Hopfinger, F. K. Browand, and Y. Gagne, Journal of Fluid Mechanics **125**, 505 (1982).
[5] L. Jacquin, O. Leuchter, C. Cambon, and J. Mathieu, Journal of Fluid Mechanics **220**, 1 (1990).
[6] C. N. Baroud, B. B. Plapp, Z.-S. She, and H. L. Swinney, Physical Review Letters **88**, 114501 (2002).
[7] C. N. Baroud, B. B. Plapp, H. L. Swinney, and Z.-S. She, Physics of Fluids **15**, 2091 (2003).
[8] C. Morize, F. Moisy, and M. Rabaud, Physics of Fluids **17** (2005).
[9] J. Bardina, J. H. Ferziger, and R. S. Rogallo, Journal of Fluid Mechanics **154**, 321 (1985).
[10] N. N. Mansour, C. Cambon, and C. G. Speziale, in *Studies in Turbulence*, edited by T. B. Gatski, S. Sarkar, and C. G. Speziale (Springer, New York, 1992), pp. 59–75.
[11] M. Hossain, Physics of Fluids **6**, 1077 (1994).
[12] P. K. Yeung and Y. Zhou, Physics of Fluids **10**, 2895 (1998).
[13] L. M. Smith and F. Waleffe, Physics of Fluids **11**, 1608 (1999).
[14] F. S. Godeferd and L. Lollini, Journal of Fluid Mechanics **393**, 257 (1999).
[15] Y. Morinishi, K. Nakabayashi, and S. Q. Ren, Physics of Fluids **13**, 2912 (2001).
[16] Q. Chen, S. Chen, G. Eyink, and D. D. Holm, Journal of Fluid Mechanics **542**, 139 (2005).
[17] K. D. Squires, J. R. Chasnov, N. N. Mansour, and C. Cambon, in *Annual Research Briefs* (Center for Turbulence Research, Stanford University, 1993), pp. 157–170.
[18] P. Bartello, O. Métais, and M. Lesieur, Journal of Fluid Mechanics **273**, 1 (1994).
[19] X. Yang and J. A. Domaradzki, Physics of Fluids **16**, 4088 (2004).
[20] H. P. Greenspan, *The theory of rotating fluids* (Cambridge University Press, Cambridge, 1968).
[21] Y. Kurihara, Monthly Weather Review **93**, 33 (1965).
[22] M. Meneguzzi and A. Pouquet, Journal of Fluid Mechanics **205**, 297 (1989).
[23] A. Vincent and M. Meneguzzi, Journal of Fluid Mechanics **225**, 1 (1991).
[24] Y. Hattori, R. Rubinstein, and A. Ishizawa, Physical Review E **70**, 046311 (2004).
[25] V. M. Canuto and M. S. Dubovikov, Physics of Fluids **9**, 2132 (1997).
[26] Y. Zhou, Physics of Fluids **7**, 2092 (1995).
[27] A.Mahalov and Y. Zhou, Physics of Fluids **8**, 2138 (1996).
[28] S. Galtier, Physical Review E **68**, 015301 (2003).
[29] C. Cambon, R. Rubinstein, and F. S. Godeferd, New Journal of Physics **6**, 73 (2004).
[30] L. M. Smith and Y. Lee, Journal of Fluid Mechanics **535**, 111 (2005).
[31] C. Cambon and L. Jacquin, Journal of Fluid Mechanics **202**, 295 (1989).
[32] C. Cambon, N. N. Mansour, and F. S. Godeferd, Journal of Fluid Mechanics **337**, 303 (1997).
[33] A. N. Kolmogorov, Proceedings of the Royal Society A **434**, 9 (1991), [Dokl. Akad. Nauk SSSR, 30(4), 1941].
[34] O. Zeman, Physics of Fluids **6**, 3221 (1994).
[35] R. Benzi, S. Ciliberto, R. Tripiccione, C. Baudet, F. Massaioli, and S. Succi, Physical Review E **48**, R29 (1993).
[36] Z.-S. She and E. Lévêque, Physical Review Letters **72**, 336 (1994).
[37] L. J. Biven, C. Connaughton, and A. C. Newell, Physica D **184**, 98 (2003).